ACS APPLIED MATERIALS & INTERFACES

Research Article

www.acsami.org

Visual Recognition of Aliphatic and Aromatic Amines Using a Fluorescent Gel: Application of a Sonication-Triggered Organogel

Xuelei Pang,[†] Xudong Yu,*[,†] Haichuang Lan,[‡] Xiaoting Ge,[†] Yajuan Li,[†] Xiaoli Zhen,[†] and Tao Yi*[,‡]

[†]College of Science and Hebei Research Center of Pharmaceutical and Chemical Engineering, Hebei University of Science and Technology, Yuhua Road 70, Shijiazhuang 050080, PR China

[‡]Department of Chemistry and Collaborative Innovation Center of Chemistry for Energy Materials, Fudan University, 220 Handan Road, Shanghai 200433, China

Supporting Information

ABSTRACT: A naphthalimide-based fluorescent gelator (**N1**) containing an alkenyl group has been designed and characterized. This material is able to gelate alcohols via a precipitate-to-gel transformation when triggered with ultrasound for less than 2 min (S-gel). The gelation process in *n*-propanol was studied by means of absorption, fluorescence, and IR spectra, scanning electron microscopy (SEM) images, and X-ray diffraction patterns. The fluorescence intensity of **N1** decreased during the gelation process in a linear relationship with the sonication time. The S-gel of **N1** could be used to sense aliphatic and aromatic amines by measuring the change in the signal output. For example, the addition of propylamine to the S-gel of **N1** resulted in a dramatic enhancement of the fluorescence intensity, accompanied by a gel-to-sol transition. On the contrary, when the S-gel of **N1** was treated with aromatic amines such as aniline, fluorescence was quenched and there was no gel collapse. The sensing mechanisms were studied by ^{1}H NMR, small-angle X-ray scattering, SEM and spectroscopic experiments. It is proposed that isomerization of the alkenyl group of **N1** from the trans to cis form occurs when the S-gel is treated with propylamine, resulting in a gel−sol transition. However, the aromatic aniline molecules prefer to insert into the gel networks of **N1** via hydrogen-bonding and charge-transfer interactions, maintaining the gel state. As potential applications, testing strips of **N1** were prepared to detect aniline.

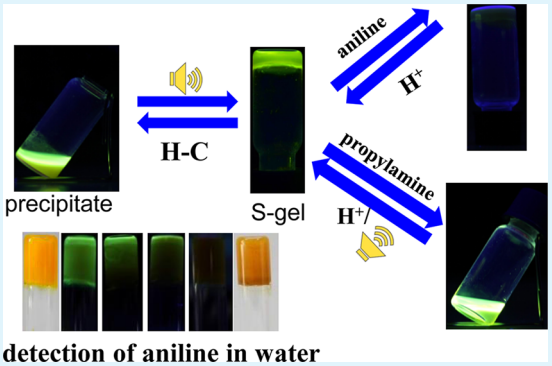

KEYWORDS: *amine sensor, fluorescence, naphthalimide, organogel, supramolecular chemistry, ultrasound*

1. INTRODUCTION

Amines and protonated amines are extensively used as intermediates in dye chemistry and are basic components of biological molecules. However, an excess of amines in the environment can be toxic, and many aromatic amines are considered to be potential carcinogens by the International Agency for the Research on Cancer.[1] The study of sensing and recognition of amines and protonated amines is therefore of great significance.[2−8] Several approaches have been developed to detect amines in the environment, such as chromatography, enzymatic methods, molecularly imprinted polymers, and molecular sensors in solution.[9−13] However, reversible, instant, and visual detection of amines still remains a major challenge, and few such applications have been reported.

Low-molar-mass organogels are supramolecular nanomaterials that have recently been developed to create sensing systems responding to important environmental stimuli including physical stimuli, such as ultrasound and shearing stress, and chemical stimuli, such as ions, pH, chiral compounds, enzymes, metal ions, and gases.[14−38] The gels can be generated by the self-assembly of gelator molecules in organic solvents or water through highly specific noncovalent interactions, such as hydrogen-bonding, hydrophobic, and electrostatic interactions, and $\pi-\pi$ stacking. They often display reversible, instant, and visual changes in response to analytes. However, very few examples of visual recognition of amines have been realized, either in solution or, particularly, in the gel state.

Fluorescence detection technology is especially attractive for visual recognition of analytes because it provides fast, real-time responses and high sensitivity and requires inexpensive equipment.[39−42] Fluorescent organogels for such applications have therefore emerged as novel and promising materials.[43−45] We have reported a series of 1,8-naphthalimide derivatives containing a cholesterol group as gelators, which are sensitive to ultrasound irradiation.[15−18] However, the practical application of these soft gels is still limited. Inspired by the concept of visual recognition, herein, we have incorporated a 2-butenedioic acid derivative into a 4-amino-1,8-naphthalimide-based gel molecule (**N1** in Scheme 1A) to generate a novel fluorescent gelator that can form a stable gel accelerated by ultrasound (S-gel), together with in situ fluorescence quenching. Because of the donor−π-acceptor (D−π-A) structural character of **N1** in

Received: April 7, 2015
Accepted: June 4, 2015
Published: June 4, 2015

DOI: 10.1021/acsami.5b03000
ACS Appl. Mater. Interfaces 2015, 7, 13569−13577

Scheme 1. (A) Chemical Structure of N1 and (B) Illustration of Ultrasound-Accelerated Gelation for Visual and Reversible Sensing of Amines

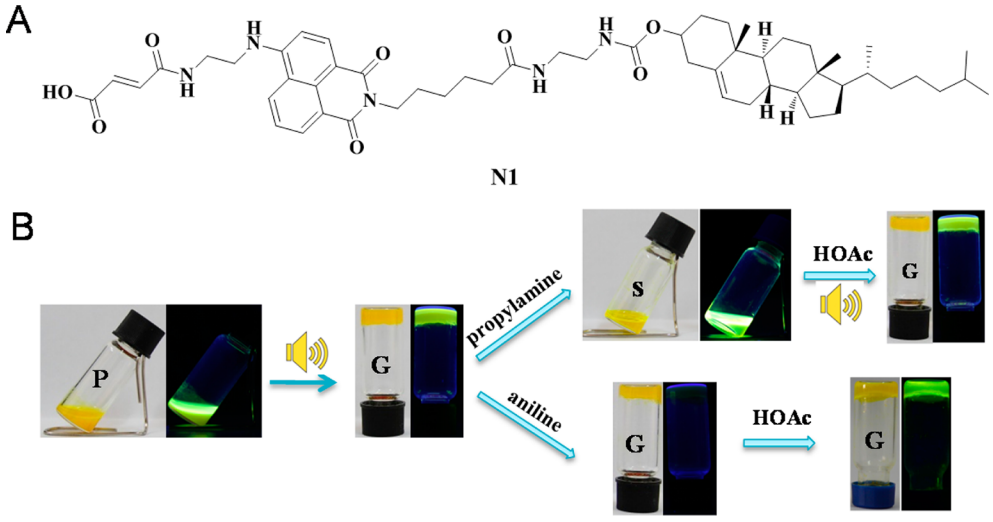

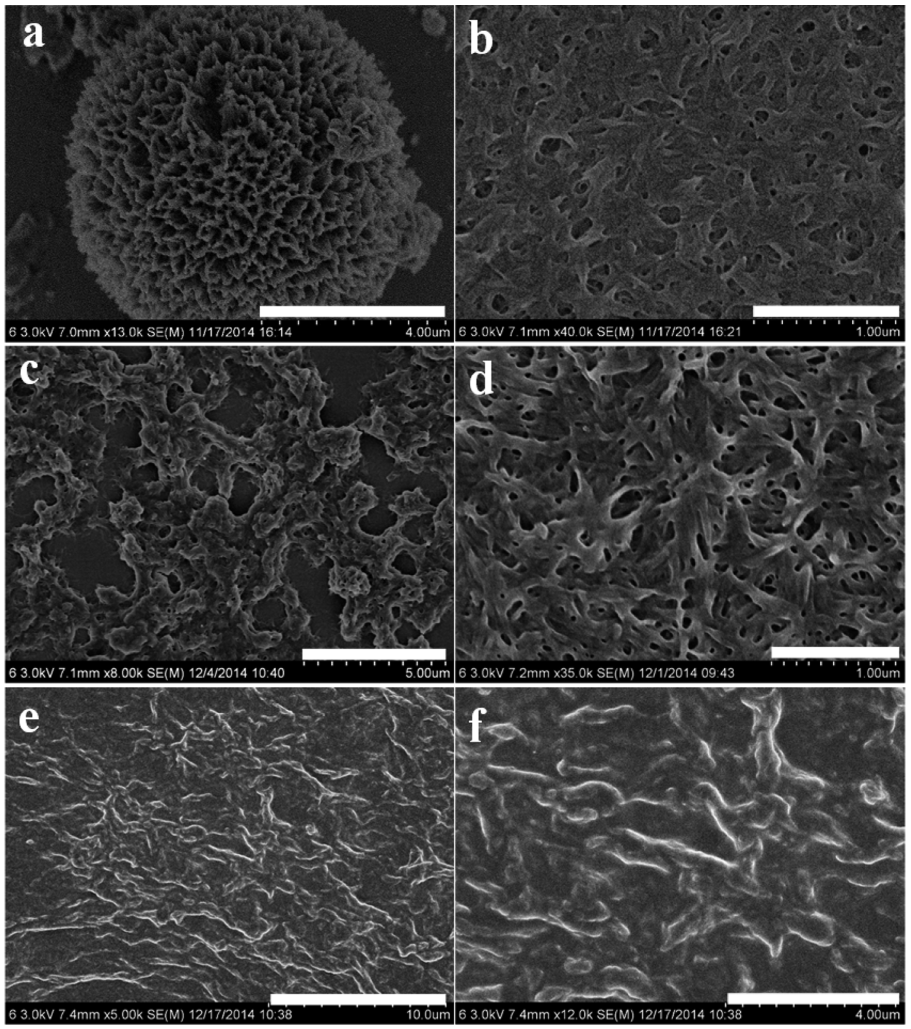

Figure 1. SEM images of **N1** S-xerogel and the gel treatment with amines: (a) precipitate of **N1** in propanol by a typical heating−cooling process; (b) S-gel of **N1** in propanol by sonication for 80 s via a direct precipitate-to-gel transition; (c) collapsing gel upon the addition of propylamine (5 equiv); (d) repaired gel by the addition of HOAc (5 equiv) followed by sonication for 2 min; (e) gel of **N1** (20 mg/mL) with aniline (10 equiv), and (f) a magnified picture of part e. [**N1**] = 20 mg/mL. Scale bar: (a) 4 μm; (b) 1 μm; (c) 5 μm; (d) 1 μm; (e) 10 μm; (f) 4 μm.

DOI: 10.1021/acsami.5b03000
ACS Appl. Mater. Interfaces 2015, 7, 13569−13577

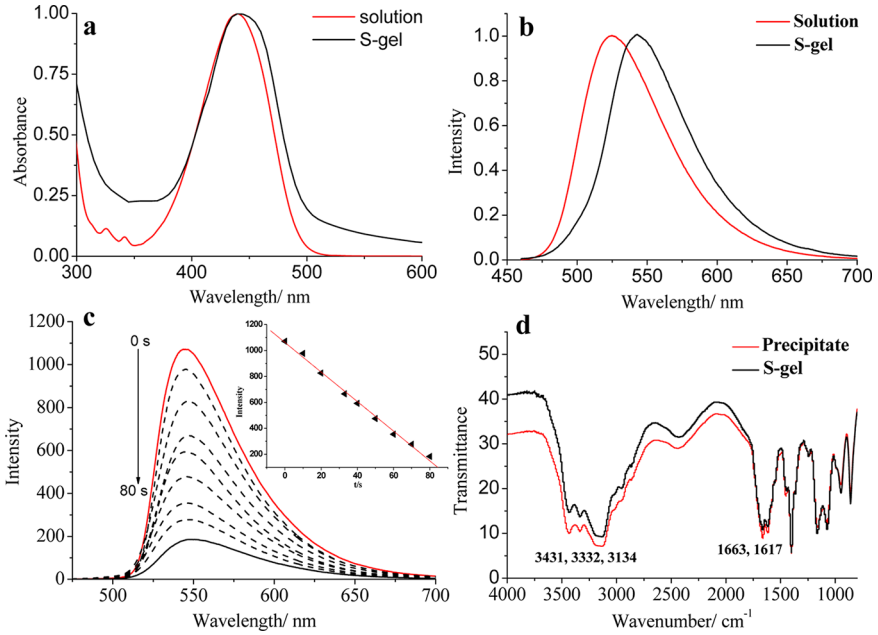

Figure 2. (a) Normalized absorption and (b) fluorescent spectra of **N1** (10^{-4} M) in solution and the gel state (20 mg/mL, 2.7×10^{-2} M). (c) Fluorescent spectral changes of **N1** via the sonication time in the process of precipitate-to-gel transformation (20 mg/mL). Inset: change of the fluorescent intensity of **N1** at 543 nm with the sonication time. (d) IR spectra of the precipitate and S-xerogel from *n*-propanol (KBr pellet).

the 1,8-naphthalimide part, fluorescence should strongly depend on the internal charge-transfer (ICT) process and the aggregation state of the fluorophore. Moreover, even though the trans conformation of the terminal alkenyl carboxylic acid would not change to a cis one at the usual conditions, the interaction between −COOH and amine may trigger the trans-to-cis conformation change of **N1**, resulting in variations of the assembly process or phase for visual recognition of amines. As expected, the gel can be used for visual and reversible recognition of organic amines, giving different signal outputs for aliphatic and aromatic amines as a result of alternate binding mechanisms in the presence of the terminal alkenyl carboxylic acid (Scheme 1B). The sensing process can also be reversed by acid and ultrasound without heating. To the best of our knowledge, this is the first example of a cholesterol-based assembly displaying visual signal outputs in response to organic amines with reversibility, which may be relevant for the design of amine sensors.

2. EXPERIMENTAL SECTION

Materials. All starting materials were obtained from commercial supplies and used without further purification. Cholesteryl chloroformate (99%) was obtained from Sigma-Aldrich. *cis*-Butenedioic anhydride (99%) was provided from Alfa Aesar. Propylamine (98.5%), 4-bromo-1,8-naphthalic anhydride (95%), aminocaproic acid, *N*-hydroxybenzotrizole (HOBt, 98%), 1-ethyl-3-[(3-(dimethylamino)-propyl]carbodiimide hydrochloride) (EDC·HCl, 98%), and other reagents were supplied from Shanghai Darui Fine Chemical Co. Ltd.

Techniques. Fourier transform infrared spectra were recorded using an IRPRESTIGE-21 spectrometer (Shimadzu). Scanning electron microscopy (SEM) images of the xerogels were obtained using SSX-550 (Shimadzu) and FE-SEM S-4800 (Hitachi) instruments. Samples were prepared by spinning the gels on glass slides and coating them with gold. NMR spectra were performed on a Bruker Advance DRX 400 spectrometer operating at 500/400 and 125/100 MHz for ^{1}H and ^{13}C NMR spectroscopy, respectively. High-resolution mass spectrometry was measured on a Bruker Micro TOF II 10257 instrument. Fluorescence spectra were collected on an Edinburgh Instruments FLS-920 spectrometer with a xenon lamp as an excitation source. Small-angle X-ray scattering (SAXS) experiments were carried out on a Nanostar U SAXS system (Bruker) at room temperature. The X-ray diffraction (XRD) pattern was generated using a Bruker AXS D8 instrument (copper target; λ = 0.1542 nm) with a power of 40 kV and 50 mA. UV−vis absorption and fluorescent spectra were recorded on a UV−vis 2550 spectroscope (Shimadzu). Sonication treatment of a sol was performed in a KQ-500DB ultrasonic cleaner (maximum power, 100 W, 40 kHz, Kunshan Ultrasound Instrument Co, Ltd., China).

3. RESULTS AND DISCUSSION

The synthesis detail of **N1** is given in the Supporting Information (SI). Gelation experiments with **N1** were carried out in 14 different solvents using a test tube inversion method.[46] The test tube (2 mL) containing **N1** and the solvent was heated to 110 °C until the solid was dissolved, and then the sample was cooled by putting it into a thermostat controlled by water (25 °C). In a typical heating−cooling process, **N1** (20 mg/mL) formed unstable gels only in toluene or benzene, which collapsed after aging for 4 h or by slight shaking. Surprisingly, the precipitate of **N1** in alcohols could transform to opaque and stable S-gels when sonicated for less than 2 min (Table S1 in the SI). The gel was tolerant to common organic solvents such as toluene, tetrahydrofuran, and acetonitrile. When the solvent was put on the top layer of the gel, neither the gel phase nor the fluorescence changed (Figure S1 in the SI). As a typical example, the properties of the **N1** gel in *n*-propanol were studied in detail.

Microstructural changes during the precipitate-to-gel transition were examined by SEM images. The precipitate of **N1** formed by a classic heating−cooling process in *n*-propanol showed a flowerlike structure on the microscale with porosity at the surface (Figures 1a and S2 in the SI). After sonication for 1 min, the flower structure was transformed into entangled fibers on the nanoscale, a typical gel structure (Figure 1b).

Comparison of the absorption and fluorescence spectra of **N1** in solution and S-gel can provide important information on the self-assembly process of **N1**. The solution (1.0×10^{-4} M)

DOI: 10.1021/acsami.5b03000
ACS Appl. Mater. Interfaces 2015, 7, 13569−13577

Scheme 2. Chemical Structures of the Tested Amines

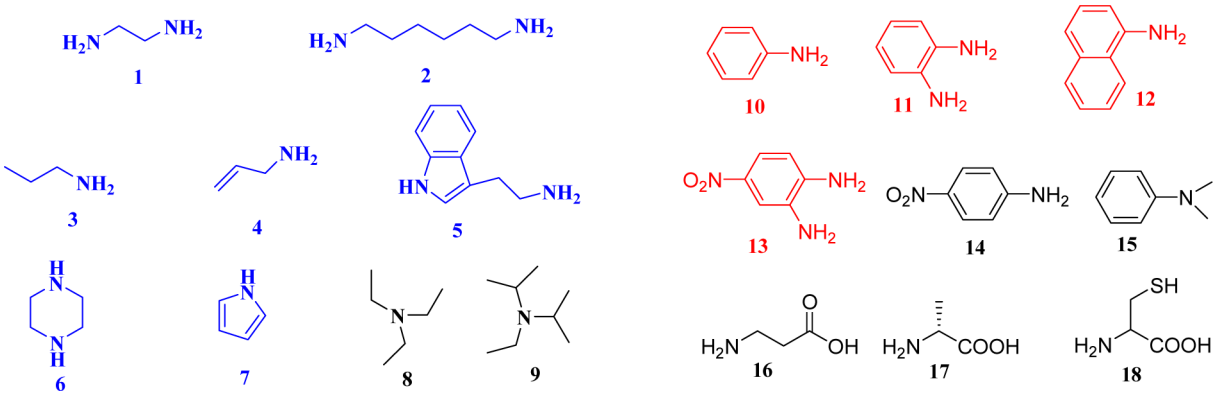

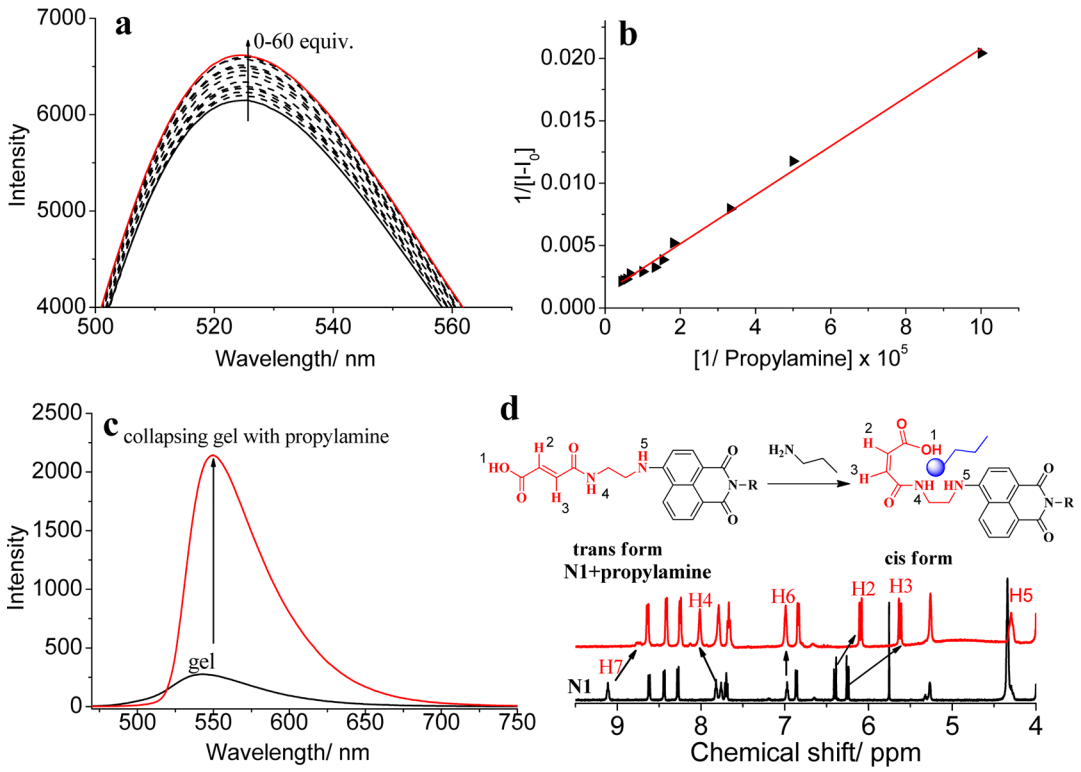

Figure 3. (a) Fluorescence titrations of **N1** in dilute solution (5×10^{-6} M) upon the addition of propylamine in propanol. (b) Reciprocal of the fluorescent intensity of **N1** (5×10^{-6} M) at 525 nm with the addition of propylamine (0−60 equiv). (c) In situ fluorescence change of the gel (20 mg/mL) upon the addition of 5 equiv of propylamine. (d) Sensing mechanism and partial ^{1}H NMR spectra of **N1** (20 mg/mL) with the addition of propylamine (5 equiv). H6 and H7 were the NH groups of amide and carbamate of **N1** in the R part, respectively.

and S-gel (20 mg/mL, 2.7×10^{-2} M) of **N1** both showed the same absorption peak at 442 nm, which was assigned to the ICT transition of the 4-imino-1,8-naphthalimide unit (Figure 2a).[47] However, the fluorescence band of the S-gel at 543 nm was 18 nm red-shifted compared to that of the solution band at 525 nm (Figure 2b), suggesting $\pi-\pi$ interactions of the **N1** molecules in the gel system.

Fluorescence control by physical stimuli is attractive because the response process is often instant, switchable, and remote. In the sonication-triggered gelation of **N1**, a regular and quantitative fluorescence quenching in response to sonication was observed. Therefore, the change in the fluorescence intensity was used to track the precipitate-to-gel transformation of **N1** in the macrostate. As seen in Figure 2c, during sonication for 0−80 s, the fluorescence intensity of the **N1** precipitate at 543 nm quenched gradually by 6-fold, suggesting that the fluorescent signal output from aggregates of **N1** molecules was very sensitive to ultrasound. The inset in Figure 2c shows a simple linear relationship of the fluorescence intensity as a function of the sonication time, with a correlation coefficient of $R^2 = 0.9976$.

We expected to find contributions from intermolecular interactions, specifically hydrogen bonds, during the gel formation. However, the precipitate and S-gel had very similar IR spectra, both showing hydrogen-bonded −NH vibrations at 3332 and 3431 cm^{-1} and C═O vibrations at 1663 and 1617 cm^{-1} (Figure 2d). A series of peaks between 2700 and 2500 cm^{-1} may suggest formation of a dimer between the carboxylic acids during the self-assembly process. To further study the molecular aggregation mechanism, SAXS experiments were

DOI: 10.1021/acsami.5b03000
ACS Appl. Mater. Interfaces 2015, 7, 13569−13577

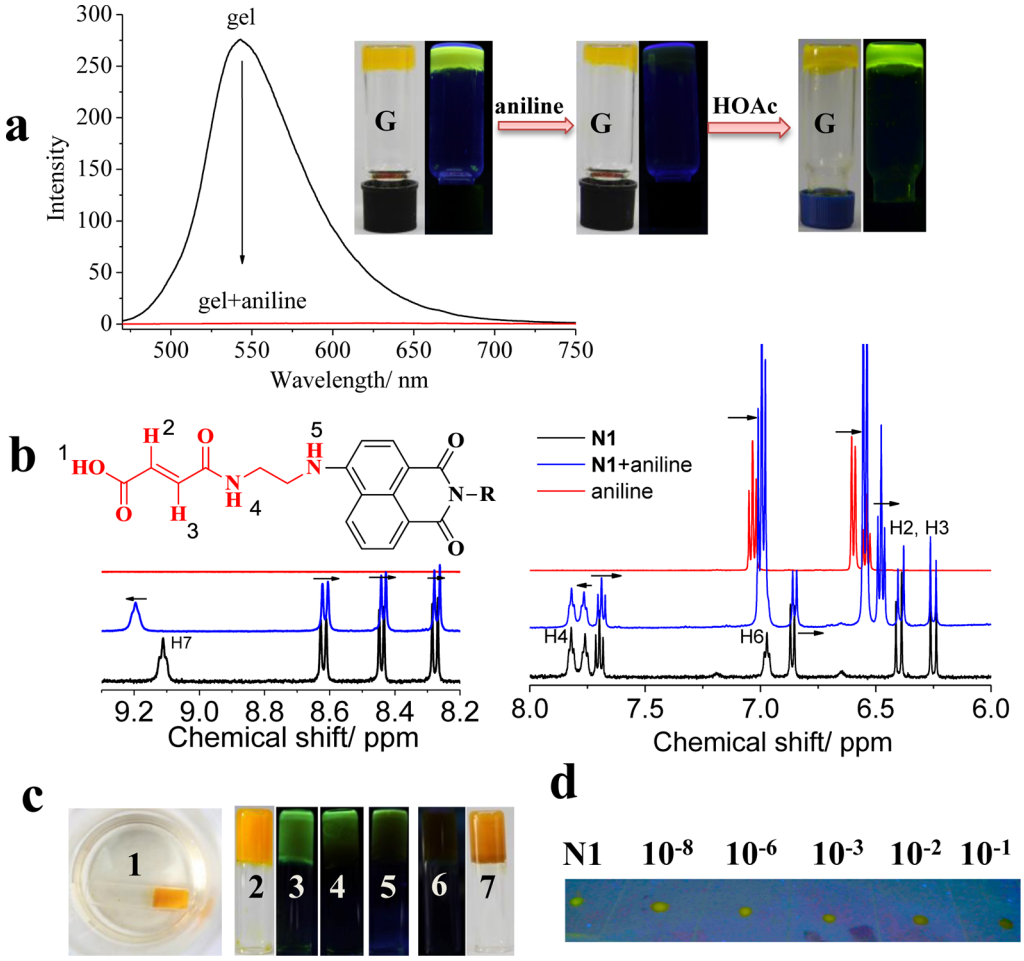

Figure 4. (a) Fluorescent spectral change of the S-gel of **N1** after aniline was captured from water (10^{-1} M). The inset contains photographs of the S-gel of **N1** with the addition of aniline and repaired by the addition of HOAc. (b) ^{1}H NMR spectra of aniline and **N1** before and after the addition of aniline (10 equiv). (c) Photographs of (1) the S-gel of **N1** capturing aniline from water (0.1 M), (2 and 3) the initial gel under day light and 365 nm light, staying for (4) 2, (5) 4, and (6–7) 8 days in the solution. (d) Detection array of a **N1** test trip toward different concentrations of aniline in aqueous solution, ranging from 10^{-1} to 10^{-8} M under UV light (365 nm).

carried out (Figure S3 in the SI). Both the precipitate and xerogel of **N1** had the same peaks at 3.9 nm in the SAXS pattern, close to twice the molecular distance, indicating a dimeric structure. These results indicate that sonication might not change the molecular aggregation mode during the self-assembly of **N1**.

The carboxylic acid group has been explored to construct two-component gels with amine derivatives through acid–base interaction.[48−52] In this context, we envisioned that the −COOH group of **N1** could interact with amines, triggering a change in the fluorescence or phase transition of the gel, providing a new type of amine-sensing system. To explore binding events between amines and **N1** in the gel state, different amines were introduced to the surfaces of the gels in *n*-propanol (compounds **1**–**18** in Scheme 2). As expected, compounds **1**–**7** (including primary aliphatic amines, secondary aliphatic amines, and pyrrole) all triggered an instant collapse of the gel. In contrast, the gel state was maintained, with high fluorescence quenching, upon the addition of aromatic amines such as aniline (**10**), *o*-diaminobenzene (**11**), 1-naphthylamine (**12**), and 4-nitro-*o*-phenylenediamine (**13**), whereas tertiary amines (**8**, **9**, and **15**), 4-nitroaniline (**14**), and amino acids (**16**–**18**) did not induce any obvious change in the gel state.

As representative examples, propylamine and aniline were chosen to study the host–guest interaction in solution and in the gel state. Upon the addition of propylamine (0–60 equiv) to a propanol solution of **N1** (5×10^{-6} M), the absorbance of **N1** was slightly increased (Figure S4 in the SI) and the fluorescence intensity at 525 nm increased by 2-fold with the addition of 60 equiv of propylamine, indicating an enhanced ICT process (Figures 3a and S5 in the SI). Plotting the fluorescence intensity change of **N1** at 525 nm as a function of 1/[propylamine] ($1/[I - I_0]$ vs 1/[propylamine]) gave a linear curve that spanned two log units, characteristic of a 1:1 binding mode (Figure 3b). The binding constant was determined to be 6.29×10^{4} M^{-1} (see details in the SI, Figure S6), and the detection limit was 1.30×10^{-7} M (Table S2 in the SI). When the S-gel of **N1** was treated with propylamine (gel concentration, 20 mg/mL; with the addition of 5 equiv of propylamine), an obvious gel–sol transition occurred. In situ fluorescence detection showed that the resulting sol displayed a 4 nm red shift from 545 to 549 nm compared with that of the gel, together with a fluorescence enhancement of 8-fold (Figure 3c), which is much higher than that observed in solution. These results revealed that the gel exhibited a signal magnification effect when sensing propylamine. Moreover, the collapse time of the gel could be controlled, ranging from seconds to

DOI: 10.1021/acsami.5b03000
ACS Appl. Mater. Interfaces 2015, 7, 13569–13577

Scheme 3. Proposed Molecular Assembly and Sensing Properties of the Gel of N1 toward Propylamine and Aniline

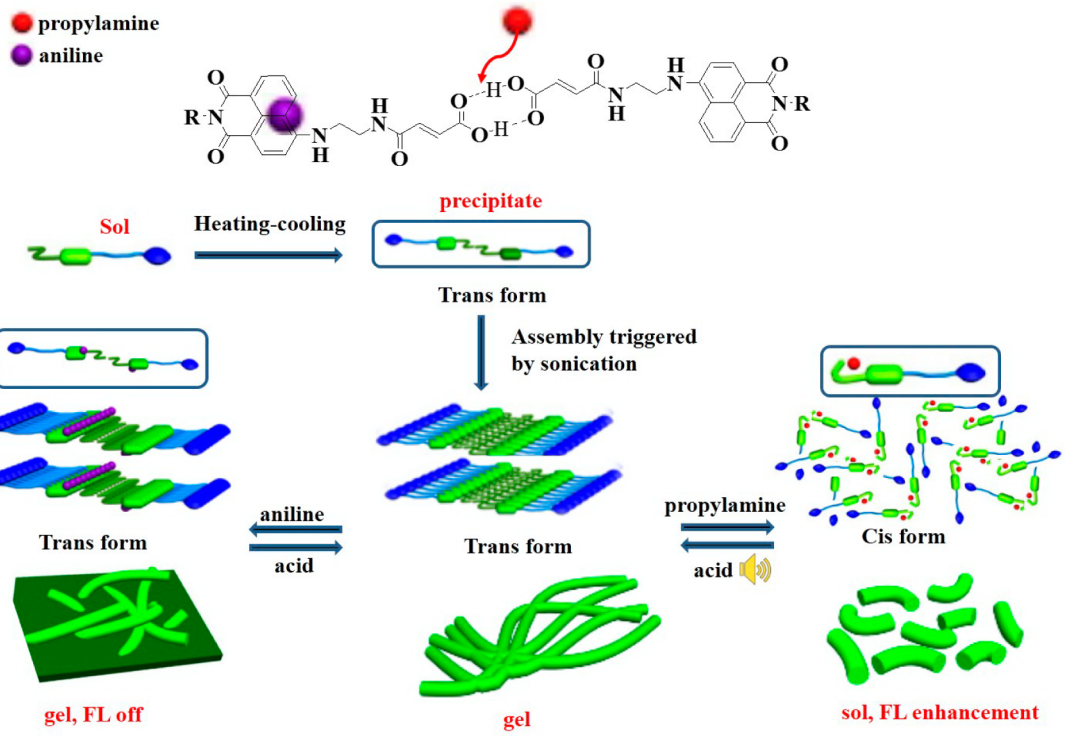

minutes, by the number of equivalents of propylamine added (Table S3 in the SI). Moreover, the gel of **N1** could even respond to vapor of amines. When the gel was put into the environment of propylamine vapor in a closed flask, the gel collapsed completely after 5 min, indicating an instant response to propylamine vapor (Figure S7 in the SI). The gel states and their fluorescent properties could be reversed to the initial state by the further addition of acid with sonication after sensing amines because the amine would be protonated in the acidic condition to destroy the acid−base interaction between **N1** and propylamine (Scheme 1B).

^{1}H NMR titrations were carried out to study the recognition of propylamine by **N1** (Figure 3d). Before the addition of propylamine, the signal of −OH(1) of the carboxylic acid did not appear in the ^{1}H NMR spectrum of **N1** because of fast proton exchange between −OH and trace water in dimethyl sulfoxide (DMSO)-d_6. However, after the addition of 5 equiv of propylamine, a new signal at 12.41 ppm was observed and might be ascribed to the active proton in the protonated propylamine (Figure S8 in the SI). Significant NMR changes of **N1** were observed on the signals for ═CH(2) and ═CH(3) of the alkenyl segment, which were shifted upfield from 6.40 and 6.24 ppm to 6.09 and 5.62 ppm, respectively, and the coupling constant was increased from J = 12.5 to 13.5 Hz, indicating that isomerization of **N1** from the trans to cis form took place. Signals from the protons of amides on NH(4) of **N1** were shifted downfield from 7.82 to 8.01 ppm in DMSO-d_6, indicating the formation of a hydrogen bond. These results suggest that **N1** first bound to propylamine via interaction between the −COOH and NH groups to form a protonated amine, which then interacted with NH(4) and NH(5) through hydrogen bonds (Figure 3d). The formation of multiple hydrogen bonds may stabilize the cis isomer of **N1**. The trans−cis conformation change of **N1** destroyed the $\pi\cdots\pi$ stacking between naphthalimide because of the enhanced steric hindrance, and the gel state was changed to solution, resulting in the enhanced fluorescence of **N1**. The upfield shifting and broadening of H(7) after the addition of propylamine was due to the formation of a hydrogen bond between excess propylamine with the carbamate −C═O group linked with NH(7). The mechanism was also confirmed by a comparison of the SAXS and powder XRD of the **N1** assembly before and after the addition of propylamine (Figure S9 in the SI). **N1** after the addition of propylamine showed no peaks in SAXS and two broadened diffractions between 2θ of 15 and 25°, indicating disordering of the collapsing gel.

The microstate changes after the gel-to-sol transition were examined by SEM. After the addition of 5 equiv of propylamine, the collapsing gel (20 mg/mL) showed a short and disordered fibrous structure (Figure 1c). Upon the further addition of propylamine to 10 equiv, nanoparticle blocking was observed, suggesting the complete destruction of **N1** aggregates (Figure S10 in the SI). The addition of an equivalent amount of HOAc followed by sonication for a few minutes restored the gel state with entangled fibers (Figure 1d).

Unlike propylamine, the addition of aniline to the **N1** gel triggered complete fluorescence quenching without phase changes (Figure 4a). The mechanism for fluorescence quenching was examined by ^{1}H NMR titration experiments in DMSO-d_6. The addition of aniline (10 equiv) resulted in a slight downfield shift of the signal for NH(7) (carbamate of **N1**) from 9.11 to 9.19 ppm, while the proton signals of the other NH groups did not show any change (Figure 4b). There was no signal of active proton observed in the low field (>10 ppm) of NMR spectra of **N1** either before or after the addition of aniline. Signals from the protons on the phenyl ring of aniline were shifted upfield by about 0.05 ppm, indicating that the aniline amine was not protonated, which may be due to the weakly basic nature of aniline (pK_b = 9.2). Proton signals from the naphthalimide group in the range of 8.7−7.5 ppm also

DOI: 10.1021/acsami.5b03000
ACS Appl. Mater. Interfaces 2015, 7, 13569−13577

showed slight upfield shifts (<0.01 ppm). Unlike what happened on **N1** with the addition of propylamine, the NMR signals of the alkenyl segment (H2 and H3) showed almost no chemical shift with the addition of aniline. The NMR data indicated weaker intermolecular interactions between **N1** and aniline. The hydrogen-bonding and $\pi-\pi$ interactions between aniline and naphthalimide may be the main reasons for fluorescence quenching of **N1** in the gel state. The fluorescence of **N1** could also be quenched by aniline in dilute solution but required 735400 equiv of aniline to quench the fluorescence intensity of **N1** (5×10^{-6} M) by 56-fold in propanol (Figure S11 in the SI). An SEM image of **N1** gel after the addition of 10 equiv of aniline showed that the fibers were transformed to a folded sheet structure, suggesting an assembly effect of aniline with **N1** molecules (Figure 1e,f). Aniline molecules may insert into the gel networks via hydrogen-bonding and charge-transfer interactions, thus accelerating fluorescence quenching of **N1** in the gel state. The SAXS pattern of xerogel of **N1** + aniline displayed a peak with a *d* value of 4.5 nm, which was larger than that of S-xerogel of **N1** (3.9 nm), suggesting that aniline was inserted into the gel assembly (Figure S9 in the SI). The peaks in the XRD pattern of **N1** + aniline were similar to that of the S-gel of **N1**, but the intensity was comparably decreased, indicating that the orderliness of the **N1** assembly was depressed to some extent.

The sensing properties of the S-gel of **N1** made it possible to detect and capture aniline in aqueous solution. For example, adding the S-gel to an aqueous aniline solution (0.1 M) and storing the resulting solution for 8 days quenched the fluorescence intensity of the S-gel by 100%, indicating the ability of the **N1** gel to absorb aniline from water. The xerogel of **N1** was also used to detect aniline in aqueous solution using testing strips prepared by putting the gel on a glass slide and drying in air to remove propanol. The slide was then placed into aqueous aniline at concentrations ranging from 10^{-1} to 10^{-8} M for 1 h and then dried in air to remove water. A simple comparison of the intensity difference enabled semiquantitative determination of aniline in aqueous solution.

From the results, the assembly and amine recognition process of **N1** can be proposed as follows (Scheme 3). By a heating−cooling process, **N1** precipitates from propanol with flowerlike morphology, adopting a dimeric structure via hydrogen-bonding interactions between the carboxylic acid groups. After sonication, **N1** can capture solvent to form a stable gel with a cross-linked nanofiber structure. The precise balance of hydrogen-bonding and hydrophobic interactions and $\pi-\pi$ stacking is the main factor in the gelation process. The addition of an aliphatic amine, such as propylamine, destroys the initial hydrogen bonding of the **N1** dimer, resulting in isomerization of **N1** from trans to cis via a hydrogen-bonding site competition effect, accompanied by a gel-to-sol transition. The fluorescence of **N1** is significantly increased in the sensing process, enabling visual recognition. In contrast, an aromatic amine such as aniline inserts into the gel network by a coassembly effect with fluorescence quenching due to $\pi-\pi$ and charge-transfer interactions between the aromatic amine and naphthalimide groups of **N1**. However, in those aromatic amines, pyrrole (7) is an exception. Even though the alkalinity of pyrrole is even weaker than that of aniline, it can collapse the gel of **N1** without a trans-to-cis transformation, as confirmed by ^{1}H NMR spectra (Figure S12 in the SI). The reason is not clear. After sensing amines in both cases, the gels and their fluorescence properties can be reversed to the initial state by the addition of acid with sonication, making the recognition events reversible.

4. CONCLUSION

In summary, this work reports an in situ and instant precipitate-to-gel formation triggered by ultrasound in a naphthalimide-based fluorescent gel at room temperature. The response of the **N1** assembly to ultrasound in propanol was accompanied by regular fluorescence quenching, which represents a new paradigm for fluorescence control by physical stimuli such as ultrasound.[50−52] The gel exhibited outstanding sensing properties for organic amines, giving opposing signal outputs in response to propylamine and aniline. To the best of our knowledge, this is the first report of the modification of ICT processes in a naphthalimide-based compound by organic amines in the gel state, providing a new strategy for the construction of amine sensors. It is suggested that hydrogen-bonding site competition between host−host (**N1**) and host−guest (amine) interactions, as well as conformational changes of the host molecules, are responsible for the recognition events. This finding clearly offers a new method for visual detection of organic amines in either a gel system or aqueous solution. Therefore, we believe that the present work will expand the real application of organogels in the fields of visual sensing and pollutant removal.

■ ASSOCIATED CONTENT

Supporting Information

Synthesis details and additional spectra. The Supporting Information is available free of charge on the ACS Publications website at DOI: 10.1021/acsami.5b03000.

■ AUTHOR INFORMATION

Corresponding Authors

*E-mail: 081022009@fudan.edu.cn.
*E-mail: yitao@fudan.edu.cn. Fax: (+86) 21-55664621.

Notes

The authors declare no competing financial interest.

■ ACKNOWLEDGMENTS

The authors are thankful for financial support from NNSFC (Grants 21125104, 21401040, 21301047, and 51373039), the Xiaoli fund SW31, Youth Foundation of Hebei Province Department of Education Fund (Grant QN2014127), Natural Science Foundation of Hebei Province (Grants B2014208160 and B2014208091), and Specialized Research Fund for the Doctoral Program of Higher Education (Grant 20120071130008).

■ REFERENCES

(1) IARC. Monograph: Overall Evaluations of Carcinogenicity to Humans, 2009. Accessed at http://monographs.iarc.fr/ENG/Classification/crthall.php on May 13, 2010.
(2) Del Blanco, S. G.; Donato, L.; Drioli, E. Development of Molecularly Imprinted Membranes for Selective Recognition of Primary Amines in Organic Medium. *Sep. Purif. Technol.* **2012**, *87*, 40−46.
(3) Purse, B. W.; Ballester, P.; Rebek, J. Reactivity and Molecular Recognition: Amine Methylation by an Introverted Ester. *J. Am. Chem. Soc.* **2003**, *125*, 14682−14683.
(4) Capici, C.; Gattuso, G.; Notti, A.; Parisi, M. F.; Pappalardo, S.; Brancatelli, G.; Geremia, S. Selective Amine Recognition Driven by

DOI: 10.1021/acsami.5b03000
ACS Appl. Mater. Interfaces 2015, 7, 13569−13577

Host−Guest Proton Transfer and Salt Bridge Formation. *J. Org. Chem.* **2012**, *77*, 9668−9675.
(5) Secor, K. E.; Glass, T. E. Selective Amine Recognition: Development of a Chemosensor for Dopamine and Norepinephrine. *Org. Lett.* **2004**, *6*, 3727−3730.
(6) Heier, P.; Förster, C.; Schollmeyer, D.; Boscher, N.; Choquetb, P.; Heinze, K. $\alpha\alpha$- and $\alpha\beta$-Zinc-*meso*-A_2B_2- Tetraarylporphyrins with Large Optical Responses to Triethylamine. *Dalton Trans.* **2013**, *42*, 906−917.
(7) Richard, J. A.; Pamart, M.; Hucher, N.; Jabin, I. Synthesis and Host−Guest Properties of a Calix[6]arene Based Receptor Closed by an Internal Ion-Paired Cap. *Tetrahedron Lett.* **2008**, *49*, 3848−3852.
(8) Zhang, X. X.; Bradshaw, J. S.; Izatt, R. M. Enantiomeric Recognition of Amine Compounds by Chiral Macrocyclic Receptors. *Chem. Rev.* **1997**, *97*, 3313−3361.
(9) García-Acosta, B.; Comes, M.; Bricks, J. L.; Kudinova, M. A.; Kurdyukov, V. V.; Tolmachev, A. I.; Descalzo, A. B.; Marcos, M. D.; Martínez-Máñez, R.; Moreno, A.; Sancenón, F.; Soto, J.; Villaescusa, L. A.; Rurack, K.; Barat, J. M.; Escriche, I.; Amorós, P. Sensory Hybrid Host Materials for the Selective Chromo- Fluorogenic Detection of Biogenic Amines. *Chem. Commun.* **2006**, 2239−2241.
(10) Özogul, F.; Taylor, K. D. A.; Quantick, P.; Özogul, Y. Changes in Biogenic Amines in Herring Stored under Modified Atmosphere and Vacuum Pack. *J. Food Sci.* **2002**, *67*, 2497−2501.
(11) Greene, N. T.; Shimizu, K. D. Colorimetric Molecularly Imprinted Polymer Sensor Array Using Dye Displacement. *J. Am. Chem. Soc.* **2005**, *27*, 5695−5700.
(12) Mohr, G. J.; Tirelli, N.; Lohse, C.; Spichiger-Keller, U. E. Development of Chromogenic Copolymers for Optical Detection of Amines. *Adv. Mater.* **1998**, *10*, 1353−1357.
(13) Babu, S. S.; Praveen, V. K.; Ajayaghosh, A. Functional π-Gelators and their Applications. *Chem. Rev.* **2014**, *114*, 1973−2129.
(14) Yu, X.; Chen, L.; Zhang, M.; Yi, T. Low-Molecular-Mass Gels Responding to Ultrasound and Mechanical Stress: Towards Self-Healing Materials. *Chem. Soc. Rev.* **2014**, *43*, 5346−5371.
(15) Wu, J.; Yi, T.; Shu, T.; Yu, M.; Zhou, Z.; Xu, M.; Zhou, Y.; Zhang, H.; Han, J.; Li, F.; Huang, C. Ultrasound Switch and Thermal Self-Repair of Morphology and Surface Wettability in a Cholesterol-Based Self-Assembly System. *Angew. Chem., Int. Ed.* **2008**, *47*, 1063−1067.
(16) Yu, X.; Liu, Q.; Wu, J.; Zhang, M.; Cao, X.; Zhang, S.; Wang, Q.; Chen, L.; Yi, T. Sonication-Triggered Instantaneous Gel-to-Gel Transformation. *Chem.—Eur. J.* **2010**, *16*, 9099−9106.
(17) Yu, X.; Cao, X.; Chen, L.; Lan, H.; Liu, B.; Yi, T. Thixotropic and Self-Healing Triggered Reversible Rheology Switching in a Peptide-based Organogel with a Cross-linked Nano-Ring Pattern. *Soft Matter* **2012**, *8*, 3329−3334.
(18) Dawn, A.; Shiraki, T.; Ichikawa, H.; Takada, A.; Takahashi, Y.; Tsuchiya, Y.; Lien, L. T. N.; Shinkai, S. Stereochemistry-Dependent, Mechanoresponsive Supramolecular Host Assemblies for Fullerenes: A Guest-Induced Enhancement of Thixotropy. *J. Am. Chem. Soc.* **2012**, *134*, 2161−2171.
(19) Huang, X.; Raghavan, S. R.; Terech, P.; Weiss, R. G. Distinct Kinetic Pathways Generate Organogel Networks with Contrasting Fractality and Thixotropic Properties. *J. Am. Chem. Soc.* **2006**, *128*, 15341−5352.
(20) Cai, X.; Wu, Y.; Wang, L.; Yan, N.; Liu, J.; Fang, X.; Fang, Y. Mechano-Responsive Calix[4]arene-Based Molecular Gels: Agitation Induced Gelation and Hardening. *Soft Matter* **2013**, *9*, 5807−5814.
(21) Komiya, N.; Muraoka, T.; Iida, M.; Miyanaga, M.; Takahashi, K.; Naota, T. Ultrasound-Induced Emission Enhancement Based on Structure-Dependent Homo- and Heterochiral Aggregations of Chiral Binuclear Platinum Complexes. *J. Am. Chem. Soc.* **2011**, *133*, 16054−16061.
(22) Xia, Q.; Mao, Y. Y.; Wu, J. C.; Shu, T. M.; Yi, T. Two-Component Organogel for Visually Detecting Nitrite Anion. *J. Mater. Chem. C* **2014**, *2*, 1854−1861.
(23) Zhang, X.; Lee, S. Y.; Liu, Y. F.; Lee, M. J.; Yin, J.; Sessler, J. L.; Yoon, J. Y. Anion-Activated, Thermoreversible Gelation System for the Capture, Release, and Visual Monitoring of CO_2. *Sci. Rep.* **2014**, *4*, 4593.
(24) Chen, X.; Huang, Z.; Chen, S. Y.; Li, K.; Yu, X. Q.; Pu, L. Enantioselective Gel Collapsing: A New Means of Visual Chiral Sensing. *J. Am. Chem. Soc.* **2010**, *132*, 7297−7299.
(25) Tu, T.; Fang, W.; Bao, X.; Li, X.; DÖtz, K. H. Visual Chiral Recognition through Enantioselective Metallogel Collapsing: Synthesis, Characterization, and Application of Platinum−Steroid Low-Molecular-Mass Gelators. *Angew. Chem., Int. Ed.* **2011**, *50*, 6601−6605.
(26) Lloyd, G. O.; Steed, J. W. Anion-Tuning of Supramolecular Gel Properties. *Nat. Chem.* **2009**, *1*, 437−442.
(27) Ren, C.; Zhang, J.; Chen, M.; Yang, Z. Self-Assembling Small Molecules for the Detection of Important Analytes. *Chem. Soc. Rev.* **2014**, *43*, 7257−7266.
(28) Yoshimura, I.; Miyahara, Y.; Kasagi, N.; Yamane, H.; Ojida, A.; Hamachi, I. Molecular Recognition in a Supramolecular Hydrogel to Afford a Semi-Wet Sensor Chip. *J. Am. Chem. Soc.* **2004**, *126*, 12204−12205.
(29) Gao, Y.; Shi, J.; Yuan, D.; Xu, B. Imaging Enzyme-Triggered Self-Assembly of Small Molecules Inside Live Cells. *Nat. Commun.* **2012**, *3*, 1033.
(30) Wang, H.; Liu, J.; Han, A.; Xiao, N.; Xue, Z.; Wang, G.; Long, J.; Kong, D.; Liu, B.; Yang, Z. Self-Assembly-Induced Far-Red/Near-Infrared Fluorescence Light-Up for Detecting and Visualizing Specific Protein−Peptide Interactions. *ACS Nano* **2014**, *8*, 1475−1484.
(31) Dey, N.; Samanta, S. K.; Bhattacharya, S. Selective and Efficient Detection of Nitro-Aromatic Explosives in Multiple Media Including Water, Micelles, Organogel, and Solid Support. *ACS Appl. Mater. Interfaces* **2013**, *5*, 8394−8400.
(32) Bhalla, V.; Gupta, A.; Kumar, M.; Shankar Rao, D. S.; Krishna Prasad, S. Self-Assembled Pentacenequinone Derivative for Trace Detection of Picric Acid. *ACS Appl. Mater. Interfaces* **2013**, *5*, 672−679.
(33) Sarkar, S.; Dutta, S.; Chakrabarti, S.; Bairi, P.; Pal, T. Redox-Switchable Copper(I) Metallogel: A Metal−Organic Material for Selective and Naked-Eye Sensing of Picric Acid. *ACS Appl. Mater. Interfaces* **2014**, *6*, 6308−6316.
(34) Zhou, S. L.; Matsumoto, S.; Tian, H. D.; Yamane, H.; Ojida, A.; Kiyonaka, S.; Hamachi, I. pH-Responsive Shrinkage/Swelling of a Supramolecular Hydrogel Composed of Two Small Amphiphilic Molecules. *Chem.—Eur. J.* **2005**, *11*, 1130−1136.
(35) Kishimura, A.; Yamashita, T.; Aida, T. Phosphorescent Organogels via "Metallophilic" Interactions for Reversible RGB−Color Switching. *J. Am. Chem. Soc.* **2005**, *127*, 179−183.
(36) Wei, S. C.; Pan, M.; Li, K.; Wang, S. J.; Zhang, J. Y.; Su, C. Y. A Multistimuli-Responsive Photochromic Metal−Organic Gel. *Adv. Mater.* **2014**, *26*, 2072−2077.
(37) Zheng, X.; Zhu, W.; Liu, D.; Ai, H.; Huang, Y.; Lu, Z. Highly Selective Colorimetric/ Fluorometric Dual-Channel Fluoride Ion Probe, and its Capability of Differentiating Cancer Cells. *ACS Appl. Mater. Interfaces* **2014**, *6*, 7996−8000.
(38) Banerjee, S.; Veale, E. B.; Phelan, C. M.; Murphy, S. A.; Tocci, G. M.; Gillespie, L. J.; Frimannsson, D. O.; Kelly, J. M.; Gunnlaugsson, T. Recent Advances in the Development of 1,8-Naphthalimide Based DNA Targeting Binders, Anticancer and Fluorescent Cellular Imaging Agents. *Chem. Soc. Rev.* **2013**, *42*, 1601−1618.
(39) Liu, B.; Tian, H. A Ratiometric Fluorescent Chemosensor for Fluoride Ions Based on a Proton Transfer Signaling Mechanism. *J. Mater. Chem.* **2005**, *15*, 2681−2686.
(40) Ashokkumar, P.; Weißhoff, H.; Kraus, W.; Rurack, K. Test-Strip-Based Fluorometric Detection of Fluoride in Aqueous Media with a BODIPY-Inked Hydrogen-Bonding Receptor. *Angew. Chem., Int. Ed.* **2014**, *53*, 2225−2229.
(41) Bhowmik, S.; Ghosh, B. N.; Marjomäki, V.; Rissanen, K. Nanomolar Pyrophosphate Detection in Water and in a Self-Assembled Hydrogel of a Simple Terpyridine-Zn^{2+} Complex. *J. Am. Chem. Soc.* **2014**, *136*, 5543−5546.
(42) Maeda, H.; Haketa, Y.; Nakanishi, T. Aryl-Substituted C_3-Bridged Oligopyrroles as Anion Receptors for Formation of

DOI: 10.1021/acsami.5b03000
ACS Appl. Mater. Interfaces 2015, 7, 13569−13577

Supramolecular Organogels. *J. Am. Chem. Soc.* **2007**, *129*, 13661−13674.
(43) Lee, J.; Kwon, J. E.; You, Y. M.; Park, S. Y. Wholly π-Conjugated Low-Molecular-Weight Organogelator That Displays Triple-Channel Responses to Fluoride Ions. *Langmuir* **2014**, *30*, 2842−2851.
(44) Murata, K.; Aoki, M.; Suzuki, T.; Harada, T.; Kawabata, H.; Komori, T.; Ohseto, F.; Ueda, K.; Shinkai, S. Thermal and Light Control of the Sol−Gel Phase Transition in Cholesterol-Based Organic Gels. Novel Helical Aggregation Modes As Detected by Circular Dichroism and Electron Microscopic Observation. *J. Am. Chem. Soc.* **1994**, *116*, 6664−6676.
(45) Duke, R. M.; Veale, E. B.; Pfeffer, F. M.; Kruger, P. E.; Gunnlaugsson, T. Colorimetric and Fluorescent Anion Sensors: An Overview of Recent Developments in the Use of 1,8-Naphthalimide-Based Chemosensors. *Chem. Soc. Rev.* **2010**, *39*, 3936−3953.
(46) Hirst, A. R.; Smith, D. K. Solvent Effects on Supramolecular Gel-Phase Materials: Two-Component Dendritic Gel. *Langmuir* **2004**, *20*, 10851−10857.
(47) Hirst, A. R.; Smith, D. K.; Feiters, M. C.; Geurts, H. P. M. Two-Component Dendritic Gel: Effect of Stereochemistry on the Supramolecular Chiral Assembly. *Chem.—Eur. J.* **2004**, *10*, 5901−5910.
(48) Suzuki, M.; Saito, H.; Hanabusa, K. Two-Component Organogelators Based on Two L-Amino Acids: Effect of Combination of L-Lysine with Various L-Amino Acids on Organogelation Behavior. *Langmuir* **2009**, *25*, 8579−8585.
(49) Chi, Z.; Zhang, X.; Xu, B.; Zhou, X.; Ma, C.; Zhang, Y.; Liu, S.; Xu, J. Recent Advances in Organic Mechanofluorochromic Materials. *Chem. Soc. Rev.* **2012**, *41*, 3878−3896.
(50) Galer, P.; Korošec, R. C.; Vidmar, M.; Šket, B. Crystal Structures and Emission Properties of the BF_2 Complex 1-Phenyl-3-(3,5-dimethoxyphenyl)-propane-1,3-dione: Multiple Chromisms, Aggregation- or Crystallization-Induced Emission, and the Self-Assembly Effect. *J. Am. Chem. Soc.* **2014**, *136*, 7383−7394.
(51) Dou, C. D.; Chen, D.; Iqbal, J.; Yuan, Y.; Zhang, H.; Wang, Y. Multistimuli-Responsive Benzothiadiazole-Cored Phenylene Vinylene Derivative with Nanoassembly Properties. *Langmuir* **2011**, *27*, 6323−6329.
(52) Liu, K.; Meng, L.; Mo, S.; Zhang, M.; Mao, Y.; Cao, X.; Huang, C.; Yi, T. Colour Change and Luminescence Enhancement in a Cholesterol-Based Terpyridyl Platinum Metallogel *via* Sonication. *J. Mater. Chem. C* **2013**, *1*, 1753−1762.

DOI: 10.1021/acsami.5b03000
ACS Appl. Mater. Interfaces 2015, 7, 13569−13577